



Tumor Necrosis Factor-Mediated Survival of CD169⁺ Cells Promotes Immune Activation during Vesicular Stomatitis Virus Infection

Prashant V. Shinde,^{a,b} Haifeng C. Xu,^{a,b} Sathish Kumar Maney,^{a,b} Andreas Kloetgen,^{c,d} Sukumar Namineni,^{e,n} Yuan Zhuang,^{a,b} Nadine Honke,^f Namir Shaabani,^g Nicolas Bellora,^h Mareike Doerrenberg,^c Mirko Trilling,ⁱ Vitaly I. Pozdeev,^{a,b} Nico van Rooijen,^j Stefanie Scheu,^k Klaus Pfeffer,^k Paul R. Crocker,^l Masato Tanaka,^m Sujitha Duggimpudi,^c Percy Knolle,ⁿ Mathias Heikenwalder,^{e,o} Jürgen Ruland,^{p,u,v,w} Tak W. Mak,^q Dirk Brenner,^{r,s} Aleksandra A. Pandya,^f Jessica I. Hoell,^c Arndt Borkhardt,^c Dieter Häussinger,^b Karl S. Lang,^f Philipp A. Lang^a

^aDepartment of Molecular Medicine II, Medical Faculty, Heinrich Heine University, Düsseldorf, Germany

^bDepartment of Gastroenterology, Hepatology, and Infectious Diseases, Heinrich-Heine-Universität Düsseldorf, Düsseldorf, Germany

^cDepartment of Pediatric Oncology, Hematology and Clinical Immunology, Center for Child and Adolescent Health, Heinrich Heine University, Medical Faculty, Düsseldorf, Germany

^dComputational Biology of Infection Research, Helmholtz Center for Infection Research, Braunschweig, Germany

^eInstitute of Virology, TU Munich, Munich, Germany

^fInstitute of Immunology, Medical Faculty, University of Duisburg-Essen, Essen, Germany

^gDepartment of Immunology and Microbial Science, The Scripps Research Institute, La Jolla, California, USA

^hInstituto Andino Patagónico de Tecnologías Biológicas y Geoambientales (IPATEC), Universidad Nacional del Comahue-CONICET, Bariloche, Argentina

ⁱInstitute for Virology of the University Hospital Essen, University of Duisburg-Essen, Essen, Germany

^jDepartment of Cell Biology, Vrije University Medical Center, Amsterdam, Netherlands

^kInstitute of Medical Microbiology and Hospital Hygiene, Heinrich-Heine-Universität Düsseldorf, Düsseldorf, Germany

^lDivision of Cell Signalling and Immunology, School of Life Sciences, University of Dundee, Dundee, United Kingdom

^mLaboratory of Immune Regulation, School of Life Science, Tokyo University of Pharmacy and Life Sciences, Tokyo, Japan

ⁿInstitute of Molecular Immunology, Technische Universität Munich and Helmholtz Zentrum Munich, Munich, Germany

^oDivision of Chronic Inflammation and Cancer, German Cancer Research Center (DKFZ), Heidelberg, Germany

^pInstitut für Klinische Chemie und Pathobiochemie, Klinikum rechts der Isar, Technische Universität Munich, Munich, Germany

^qPrincess Margaret Cancer Center, University Health Network, Toronto, Ontario, Canada

^rDepartment of Infection and Immunity, Experimental and Molecular Immunology, Luxembourg Institute of Health, Esch-sur-Alzette, Luxembourg

^sOdense Research Center for Anaphylaxis (ORCA), Department of Dermatology and Allergy Center, Odense University Hospital, University of Southern Denmark, Odense, Denmark

^tDepartment of Rheumatology, Hiller Research Center Rheumatology, Heinrich-Heine-Universität Düsseldorf, Düsseldorf, Germany

^uGerman Cancer Consortium (DKTK), partner site Munich, Germany

^vGerman Center for Infection Research (DZIF), partner site Munich, Germany

^wCenter for Translational Cancer Research (TranslaTUM), Technical University of Munich, Munich, Germany

ABSTRACT Innate immune activation is essential to mount an effective antiviral response and to prime adaptive immunity. Although a crucial role of CD169⁺ cells during vesicular stomatitis virus (VSV) infections is increasingly recognized,

Received 19 September 2017 Accepted 1 November 2017

Accepted manuscript posted online 15 November 2017

Citation Shinde PV, Xu HC, Maney SK, Kloetgen A, Namineni S, Zhuang Y, Honke N, Shaabani N, Bellora N, Doerrenberg M, Trilling M, Pozdeev VI, van Rooijen N, Scheu S, Pfeffer K, Crocker PR, Tanaka M, Duggimpudi S, Knolle P, Heikenwalder M, Ruland J, Mak TW, Brenner D, Pandya AA, Hoell JI, Borkhardt A, Häussinger D, Lang KS, Lang PA. 2018. Tumor necrosis factor-mediated survival of CD169⁺ cells promotes immune activation during vesicular stomatitis virus infection. *J Virol* 92:e01637-17. <https://doi.org/10.1128/JVI.01637-17>.

Editor Bryan R. G. Williams, Hudson Institute of Medical Research

Copyright © 2018 Shinde et al. This is an open-access article distributed under the terms of the [Creative Commons Attribution 4.0 International license](https://creativecommons.org/licenses/by/4.0/).

Address correspondence to Philipp A. Lang, langp@uni-duesseldorf.de.

K.S.L. and P.A.L. contributed equally to this work.

factors regulating CD169⁺ cells during viral infections remain unclear. Here, we show that tumor necrosis factor is produced by CD11b⁺ Ly6C⁺ Ly6G⁺ cells following infection with VSV. The absence of TNF or TNF receptor 1 (TNFR1) resulted in reduced numbers of CD169⁺ cells and in reduced type I interferon (IFN-I) production during VSV infection, with a severe disease outcome. Specifically, TNF triggered RelA translocation into the nuclei of CD169⁺ cells; this translocation was inhibited when the paracaspase MALT-1 was absent. Consequently, MALT1 deficiency resulted in reduced VSV replication, defective innate immune activation, and development of severe disease. These findings indicate that TNF mediates the maintenance of CD169⁺ cells and innate and adaptive immune activation during VSV infection.

IMPORTANCE Over the last decade, strategically placed CD169⁺ metallophilic macrophages in the marginal zone of the murine spleen and lymph nodes (LN) have been shown to play a very important role in host defense against viral pathogens. CD169⁺ macrophages have been shown to activate innate and adaptive immunity via “enforced virus replication,” a controlled amplification of virus particles. However, the factors regulating the CD169⁺ macrophages remain to be studied. In this paper, we show that after vesicular stomatitis virus infection, phagocytes produce tumor necrosis factor (TNF), which signals via TNFR1, and promote enforced virus replication in CD169⁺ macrophages. Consequently, lack of TNF or TNFR1 resulted in defective immune activation and VSV clearance.

KEYWORDS TNF, MALT1, innate immunity, interferon, NF- κ B, innate immunity, interferons, tumor necrosis factor

Innate immune activation is crucial for inducing antiviral immunity through cytokine production and adaptive immune priming (1). Splenic marginal-zone macrophages and metallophilic marginal-zone macrophages play an important role in eliminating blood-borne bacteria, parasites, and viral pathogens (2, 3). Metallophilic macrophages were originally described when rat splenic marginal-zone macrophages were stained by iron and silver impregnation (4). These metallophilic macrophages express the lectin-like hemagglutinin CD169, which was identified using a monoclonal antibody, MOMA-1 (5–7). CD169⁺ macrophages are increasingly recognized to play a pivotal role in host defense (8). CD169⁺ macrophages (referred to here as CD169⁺ cells), specifically allow early viral replication to promote innate immune recognition and antigen presentation (9). The absence of CD169⁺ cells results in reduced type I interferon (IFN-I) production, reduced B-cell activation, and development of severe disease during viral infection (10, 11). B-cell-derived lymphotoxin alpha (Lt α) and lymphotoxin beta (Lt β) drive the maintenance of CD169⁺ cells in spleen and lymph node tissue (10, 12, 13). Consequently, B-cell-deficient mice exhibit fewer CD169⁺ cells and limited immune activation, including the production of IFN-I (13, 14). However, the factors promoting survival and the presence of CD169⁺ cells after viral infection have not yet been sufficiently studied.

IFN-I triggers strong inhibitory effects on viral replication and is crucial for preventing severe infections with the vesicular stomatitis virus (VSV) model system (1, 15). This system can be used as a laboratory system for immune recognition during viral infection, as a vaccine vector system, as a tool for viral transduction, and as an oncolytic virus (16, 17). Clearance of VSV depends heavily on IFN-I and the presence of neutralizing antibodies (15, 18). VSV has been used as a murine model of viral infections to study the innate immune response and virus replication in secondary lymphoid organs and the central nervous system (CNS) (19–21). Pathology in VSV infection is seen particularly during infection of the CNS; this pathology includes paralysis and death after infection with VSV (22). Accordingly, mice deficient in IFN- α/β receptor (IFNAR) signaling exhibit paralysis and the presence of VSV in the CNS (15). Consistently, IFN-I can inhibit VSV replication in neurons, and defects in IFN-stimulated genes (ISGs) in the CNS tissue trigger pathology during VSV infection (23, 24). During infection with low

doses of VSV, replication of VSV in CD169⁺ cells in the spleen and lymph node tissue is important for inducing protective immunity and preventing CNS infection (9, 10). The VSV backbone is also used during vaccination to induce protective immunity against viruses such as Ebola virus (25).

The role of tumor necrosis factor (TNF) in marginal-zone development and marginal-zone function is controversial. Although reports show that marginal-zone development is impaired and fewer marginal-zone macrophages are present in TNF-deficient and p55-TNFR (tumor necrosis factor receptor 1 [TNFR1])-deficient mice (26), other reports suggest that TNF triggers marginal-zone macrophage depletion after infection (27, 28). It has also been shown that TNFR1-deficient mice are less susceptible to West Nile virus infection as a result of an uncompromised blood-brain barrier (29). However, other studies utilizing herpes simplex virus 1 as an infection model showed that TNFR1-deficient mice are more susceptible to virus infection (30, 31). It is clear that TNF-deficient mice exhibit CD169⁺ cells in the spleen, whereas this cell population is absent in *Ltα*^{-/-} mice (26, 27). Furthermore, the production of neutralizing antibodies and the proliferation of antiviral T cells can be induced in TNF-deficient animals (28, 32). These findings suggest that TNF, which is crucial for overcoming bacterial infections (33–36), plays a minor role in antiviral immunity.

In this study, we found that absence of TNF reduced the number of CD169⁺ cells; inhibited IFN- γ production; and, consequently, led to a severe disease outcome during infection with VSV. These effects were mainly transmitted by TNFR1 and were dependent on canonical nuclear factor κ B (NF- κ B).

RESULTS

TNF production by CD11b⁺ Ly6C⁺ Ly6G⁺ cells following VSV infection. TNF can be detected during an infection with VSV (32, 37). Consistently, we found that TNF expression levels were higher in the spleen after infection with VSV than in uninfected controls (Fig. 1A). Backgating of intracellular-TNF-producing cells showed that TNF-producing cells are a heterogeneous CD11b⁺ CD19⁻ population (Fig. 1B and C). Therefore, we hypothesized that TNF was likely not expressed by B or T cells during infection. Accordingly, we observed TNF mRNA expression levels in *Cd8*^{-/-}, B-cell-deficient *Jh*^{-/-}, and *Rag1*^{-/-} mice that were comparable to those in wild-type (WT) mice (Fig. 1D). TNF-producing cells could be predominantly characterized as CD11b⁺ CD11c⁻ Ly6C⁺ Ly6G⁺ major histocompatibility complex class II negative (MHC-II⁻) (Fig. 1E). Consistent with reports that neutrophils (38, 39) and CD11b⁺ Ly6C⁺ Ly6G⁺ cells (40) are important during early defense against bacterial and viral infections via production of proinflammatory cytokines, such as interleukin 1b (IL-1b), IL-6, TNF, and IFN- γ , we found a significant increase of TNF⁺ CD11b⁺ Ly6C⁺ Ly6G⁺ cells (Fig. 1F). Treatment with clodronate encapsulated in liposomes (clodronate liposomes) can deplete phagocytic cells in mice (Fig. 1G) (41, 42). Accordingly, clodronate depletion reduced TNF expression after VSV infection, suggesting a role of these phagocytic cells in the production of TNF (Fig. 1H). However, when we employed diphtheria toxin receptor (DTR)-induced specific depletion of CD169⁺ cells and CD11c⁺ cells, we did not observe a reduction in TNF production (Fig. 1H). Taken together, these findings indicate that TNF production following intravenous VSV infection is triggered by CD11b⁺ CD11c⁻ Ly6C⁺ Ly6G⁺ phagocytes.

TNF triggers the maintenance of CD169⁺ cells during viral infection to protect animals against the development of severe disease. To determine whether TNF affects the outcome after VSV infection, we infected WT and TNF-deficient mice. TNF-deficient mice developed severe VSV infection in comparison to WT mice (Fig. 2A). A neutralizing antibody titer was achieved later in TNF-deficient mice than in WT mice after infection with low doses of VSV (Fig. 2B). Since IFN- γ is critical to overcome an infection with VSV (15), we measured IFN- α and IFN- β in the sera of infected animals. IFN- α production was impaired in TNF-deficient mice compared to control animals (Fig. 2C). However, IFN- β was undetectable in the sera of animals infected with 10⁵ PFU VSV (Fig. 2C). Previous findings showed that CD169⁺ cells contribute to innate immune

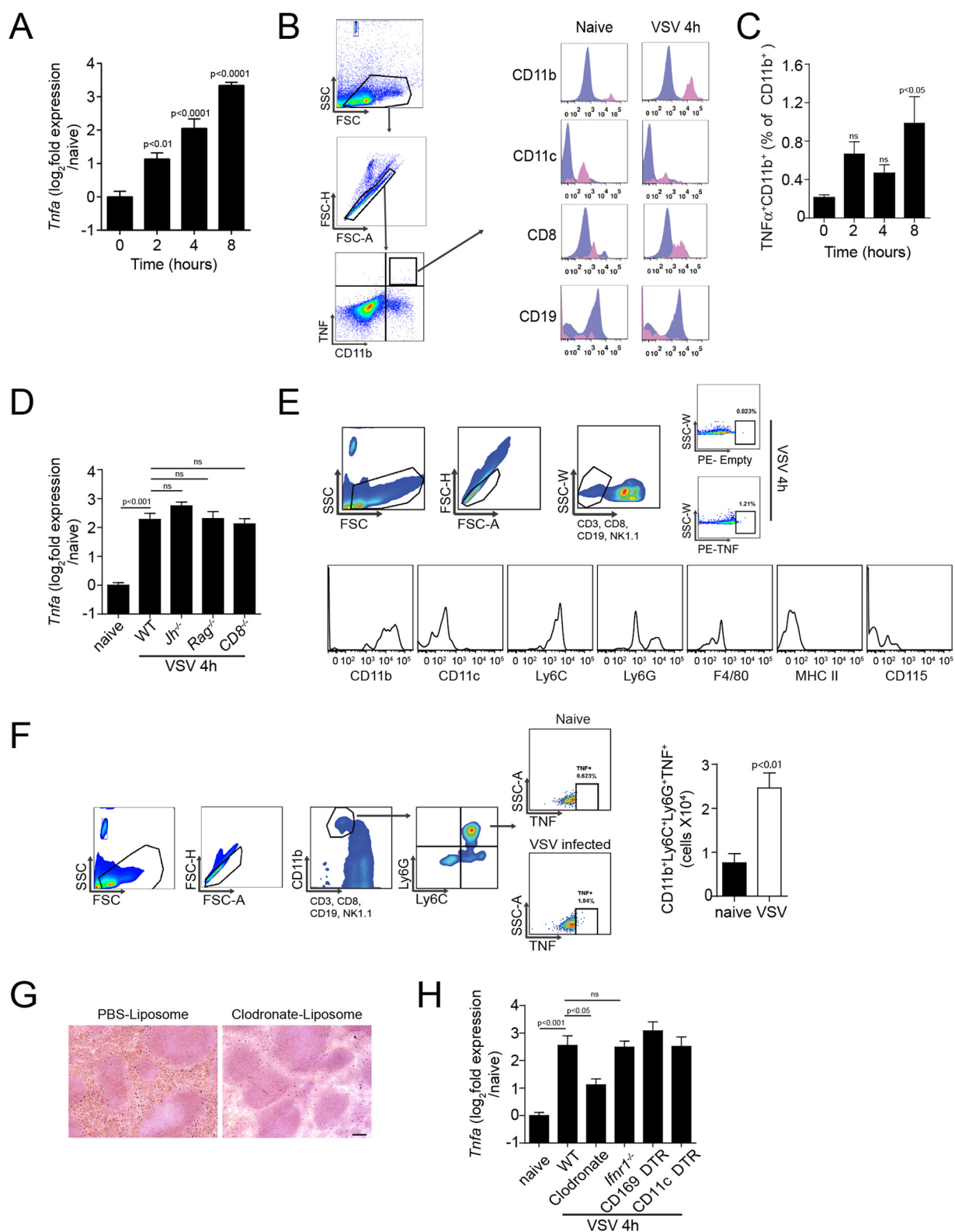


FIG 1 Vesicular stomatitis virus infection leads to infiltration of TNF-producing phagocytes. (A to F) WT mice were infected with 2×10^8 PFU VSV. (A) TNF- α mRNA expression levels in WT spleen tissue were determined at the indicated time points after infection ($n = 4$ to 10). (B) Surface molecule expression of CD11b, CD11c, CD8, and CD19 on TNF⁺ cells 4 h after infection (purple gate, whole spleen; pink gate, TNF⁺ cells; one representative result out of 5 is shown). Numbers below the histograms indicate fluorescence intensities. FSC, forward scatter; SSC, side scatter. (C) Splenocytes from WT mice were stained for intracellular-TNF production. TNF⁺ CD11b⁺ cells were determined as percentages of total CD11b⁺ cells ($n = 5$). (D) TNF- α mRNA expression in the spleens of WT, *Jh*^{-/-}, *Rag*^{-/-}, and *CD8*^{-/-} mice was determined 4 h after infection ($n = 5$ or 6). (E) Surface molecule expression of TNF-producing cells 4 h after infection. CD3⁻ CD8⁻ CD19⁻ NK1.1⁻ cells were further characterized for

(Continued on next page)

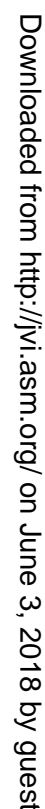
activation in mice, not only by allowing viral replication, but also by producing IFN-I (10, 43). When we depleted CD169⁺ cells expressing diphtheria toxin receptor (CD169-DTR cells) by administering diphtheria toxin (DT) (44), we observed reduced IFN-I concentrations in the sera of infected animals (Fig. 2D). To exclude the possibility of defective innate Toll-like receptor (TLR) activation, we administered the TLR3 agonist poly(I-C). We found that the IFN-I production was intact in both WT and TNF-deficient mice (Fig. 2E). Hence, we speculated that TNF promoted the function of CD169⁺ cells and thus contributed to IFN-I production following VSV infection. Shortly after infection with VSV, the number of CD169⁺ cells in spleen tissue decreased in TNF-deficient mice compared to spleen tissue harvested from WT animals (Fig. 2F to H). To understand the reduced production of IFN-I in the absence of TNF, we monitored the virus replication in spleen tissue of WT and *Tnfa*^{-/-} mice. The expression of VSV glycoprotein (VSV-G) was detected in smaller quantities in spleen tissue harvested from TNF-deficient animals than in spleen tissue harvested from WT mice after VSV infection (Fig. 2I and J). Consistently, early VSV titers after infection were lower in *Tnfa*^{-/-} mice than in control mice, a condition that negatively affected antiviral immune activation (Fig. 2K). Injection of UV light (UV)-inactivated virus could increase TNF mRNA expression in WT mice (Fig. 2L). However, the decrease of CD169⁺ cells was dependent on live virus, because UV-inactivated virus did not affect CD169⁺ cells in spleen tissue of *Tnfa*^{-/-} mice (Fig. 2M). These findings indicate that TNF is necessary to sustain virus replication in the early hours of infection but is dispensable for sterile innate immune activation. Notably, *CD169*^{-/-} mice exhibited VSV-G expression in spleen tissue, a finding indicating that downregulation of the protein CD169 would not cause absence of virus replication (Fig. 2N). Taken together, these findings indicate that the absence of TNF results in defective antiviral innate immune activation after infection with VSV.

CD169⁺ cell maintenance via TNFR1 results in productive VSV replication and immune activation. To further characterize the role of TNF during viral infection, we infected TNFR1- and TNFR2-deficient mice with VSV. In line with findings from TNF-deficient animals, the absence of TNFR1, but not that of TNFR2, resulted in a decrease in the number of CD169⁺ cells in spleen tissue (Fig. 3A and B). Furthermore, VSV-G production was lower in *Tnfrsf1a*^{-/-} animals than in WT or *Tnfrsf1b*^{-/-} mice (Fig. 3A). Consistently, VSV titers were reduced in spleen tissue shortly after infection in *Tnfrsf1a*^{-/-} animals, in sharp contrast to the findings in WT and *Tnfrsf1b*^{-/-} mice (Fig. 3C). Interestingly, IFN-I production was defective in *Tnfrsf1a*^{-/-} mice but was also lower in *Tnfrsf1b*^{-/-} animals than in WT control mice (Fig. 3D). IFN-I is necessary for the expression of antivirally active ISGs (1). Consistently, we found reduced expression of ISGs in the CNS of *Tnfrsf1a*^{-/-} mice after infection with VSV (Fig. 3E). Defective ISG expression was not found to the same extent in *Tnfrsf1b*^{-/-} CNS tissue (Fig. 3F). VSV can drive neuropathological symptoms by infecting the CNS (22). When we measured viral titers in the spinal cord and brain tissue of mice exhibiting hind leg paralysis, we found infectious VSV in tissue from TNFR1-deficient mice (Fig. 3G). Consequently, *Tnfrsf1a*^{-/-} mice developed clinical signs of CNS infection, unlike WT and *Tnfrsf1b*^{-/-} mice (Fig. 3H). Taken together, these findings suggest that TNFR1 drives antiviral defense by promoting CD169⁺ cell survival.

TNFR1 triggers the survival of CD169⁺ cells. Next, we opted to determine which factors drive the maintenance of CD169⁺ cells and enforced viral replication after viral infection. B-cell-mediated Lt β production is important for splenic CD169⁺ cells. Hence, we wondered whether the defects in the absence of TNF were triggered by B cells.

FIG 1 Legend (Continued)

expression of CD11b, CD11c, Ly6C, Ly6G, F4/80, MHC-II, and CD115 on TNF⁺ cells ($n = 6$). The numbers in the boxes are percentages of the population positive for TNF expression. (F) CD3⁻ CD8⁻ CD19⁻ NK1.1⁻ CD11b⁺ Ly6C⁺ Ly6G⁺ TNF⁺ cells were quantified in spleen tissue 4 h after infection ($n = 6$). (G) Mice were injected with liposomes containing phosphate-buffered saline (PBS; PBS liposomes) or clodronate liposomes, and spleen tissue was harvested after 24 h. Sections of snap-frozen spleen tissue were stained with anti-F4/80 antibodies ($n = 3$). (H) TNF- α mRNA expression was determined in the spleens of WT, clodronate-treated WT, *lfnar*^{-/-}, DT-treated CD169-DTR, and CD11c-DTR mice 4 h after infection ($n = 6$). ns, not significant. The error bars indicate SEM.



(Continued on next page)

Notably, we did not observe any major changes of B-cell subsets in TNF^{-/-}, TNFR1^{-/-}, or TNFR2-deficient mice (Fig. 4A). Consistently, we did not see differential expression of *Ltα*, *Ltβ*, or *Ltβ* receptor (*LtβR*) in TNFR1-deficient mice (Fig. 4B). Additionally, we found no major differences in B-cell subsets between WT and *Tnfrsf1a*^{-/-} mice after infection (Fig. 4C). Furthermore, we reconstituted lethally irradiated C57BL/6 mice with mixed bone marrow (BM) from *Rag1*^{-/-} and *Tnfrsf1a*^{-/-} and from *Rag1*^{-/-} and WT donors at a ratio of 1:1. Mice reconstituted with *Rag1*^{-/-}-*Tnfrsf1a*^{-/-} bone marrow exhibited no significant reduction in IFN-α in the serum compared to mice reconstituted with *Rag1*^{-/-}-WT bone marrow (Fig. 4D). Furthermore, there was no difference between these mice in neutralizing antibody production (Fig. 4E). To elucidate if TNFR1 deficiency specifically on CD169⁺ cells has a role in virus replication, we reconstituted lethally irradiated C57BL/6 mice with mixed bone marrow from CD169-DTR⁺ and *Tnfrsf1a*^{-/-} donors, as well as CD169-DTR⁺ and WT donors, at a ratio of 1:1. We observed that the production of IFN-α was lower in the mice reconstituted with CD169-DTR⁺ and *Tnfrsf1a*^{-/-} bone marrow compared to control mice reconstituted with CD169-DTR⁺ and WT bone marrow after infection with VSV and DT treatment (Fig. 4F). Furthermore, we found slightly delayed presence of VSV neutralizing antibody titers in CD169-DTR⁺-*Tnfrsf1a*^{-/-} recipients compared to corresponding CD169-DTR⁺-WT recipients (Fig. 4G). CD169⁺ cells can be depleted in CD11c-DTR mice, because CD169⁺ cells exhibit intermediate expression of CD11c (10, 45). Consistently, lethally irradiated mice reconstituted with mixed bone marrow from CD11c-DTR⁺ and *Tnfrsf1a*^{-/-} mice exhibited reduced concentrations of IFN-α after VSV infection compared to CD11c-DTR⁺-WT bone marrow recipients (Fig. 4H). These findings suggest that TNFR1 triggers cell-intrinsic effects on CD169⁺ cells.

We speculated that TNF delivers an important survival signal for CD169⁺ cells. To determine if TNF is involved in protection against VSV-induced apoptosis, we measured caspase 3 activity on whole spleen tissue lysates. After VSV infection, caspase 3 activity was significantly higher in *Tnfa*^{-/-} mice than in control animals (Fig. 5A). VSV is known to induce apoptosis and inactivates Mcl-1 and Bcl-XL (46). To elucidate if TNF plays a role in promoting expression of antiapoptotic genes, we measured mRNA expression of *Bcl2*, *Bcl-XL*, and *xIAP* in spleen tissue of mice after VSV infection (Fig. 5B). After VSV infection, *Bcl2* and *Bcl-XL* expression was significantly reduced in *Tnfa*^{-/-} mice compared to WT mice (Fig. 5B). To enumerate the mechanism that reduces CD169⁺ cells in TNF-deficient mice after infection, we made use of terminal deoxynucleotidyltransferase-mediated dUTP-biotin nick end labeling (TUNEL) assays. The number, as well as the mean fluorescence intensity, of TUNEL-positive CD169⁺ cells was higher in spleen tissue from TNF-deficient mice than in tissue from corresponding WT control mice (Fig. 5C and D). The proportion of CD169⁺ cells that stained positive for 7-aminoactinomycin D (7-AAD) was higher in TNFR1-deficient mice than in WT control mice 8 h after infection (Fig. 5E). Next, we wondered if we could rescue the CD169⁺ cells by injecting the pancaspase inhibitor Z-Val-Ala-Asp-fluoromethylketone (Z-VAD). Z-VAD treatment restored the presence of CD169⁺ cells in TNF-deficient animals, a finding indicating that CD169⁺ cells depend on TNF-mediated survival (Fig. 5F and G). Although treatment of TNF-deficient mice with Z-VAD-rescued CD169⁺ cells, it failed to rescue the IFN-I response, suggesting the role of TNF signaling is essential not only to prevent apoptosis, but also for IFN-I production (Fig. 5H). In summary, these findings indicate that TNF delivers a survival signal that is important for the maintenance of CD169⁺ cells in the spleen after viral infection and for IFN-I production.

FIG 2 Legend (Continued)

per spleen from 3 or 4 mice were analyzed). (H) MFI from *Tnfa*^{-/-} mice normalized to WT MFI. (I) Snap-frozen spleen sections from WT and *Tnfa*^{-/-} mice were stained for VSV-G expression (clone Vi10) after infection with 2×10^8 PFU VSV at the indicated time points (one representative result out of 6 mice is shown; scale bar = 100 μm). (J) MFI of VSV-G expression quantified across spleen sections from naive and VSV-infected WT and *Tnfa*^{-/-} mice using ImageJ (1 to 3 images per spleen from 3 or 4 mice were analyzed). (K) WT and *Tnfa*^{-/-} mice were infected with 10^5 PFU VSV. Viral titers were measured in the spleens of WT and *Tnfa*^{-/-} mice 8 h after infection with VSV ($n = 6$). (L) *Tnfa* mRNA expression determined in spleen tissue of WT mice before and 4 h after injection with UV-inactivated VSV ($n = 4$). (M) Spleen tissue sections were stained with anti-CD169 antibodies in WT and *Tnfa*^{-/-} mice 8 h after infection with 2×10^8 PFU of UV-inactivated VSV (one representative result out of 3 is shown). (N) Sections from snap-frozen spleen tissue harvested from WT and *CD169*^{-/-} mice were stained for CD169 and VSV-G 7 h after infection with 2×10^8 PFU VSV ($n = 3$; scale bar = 100 μm). The error bars indicate SEM.

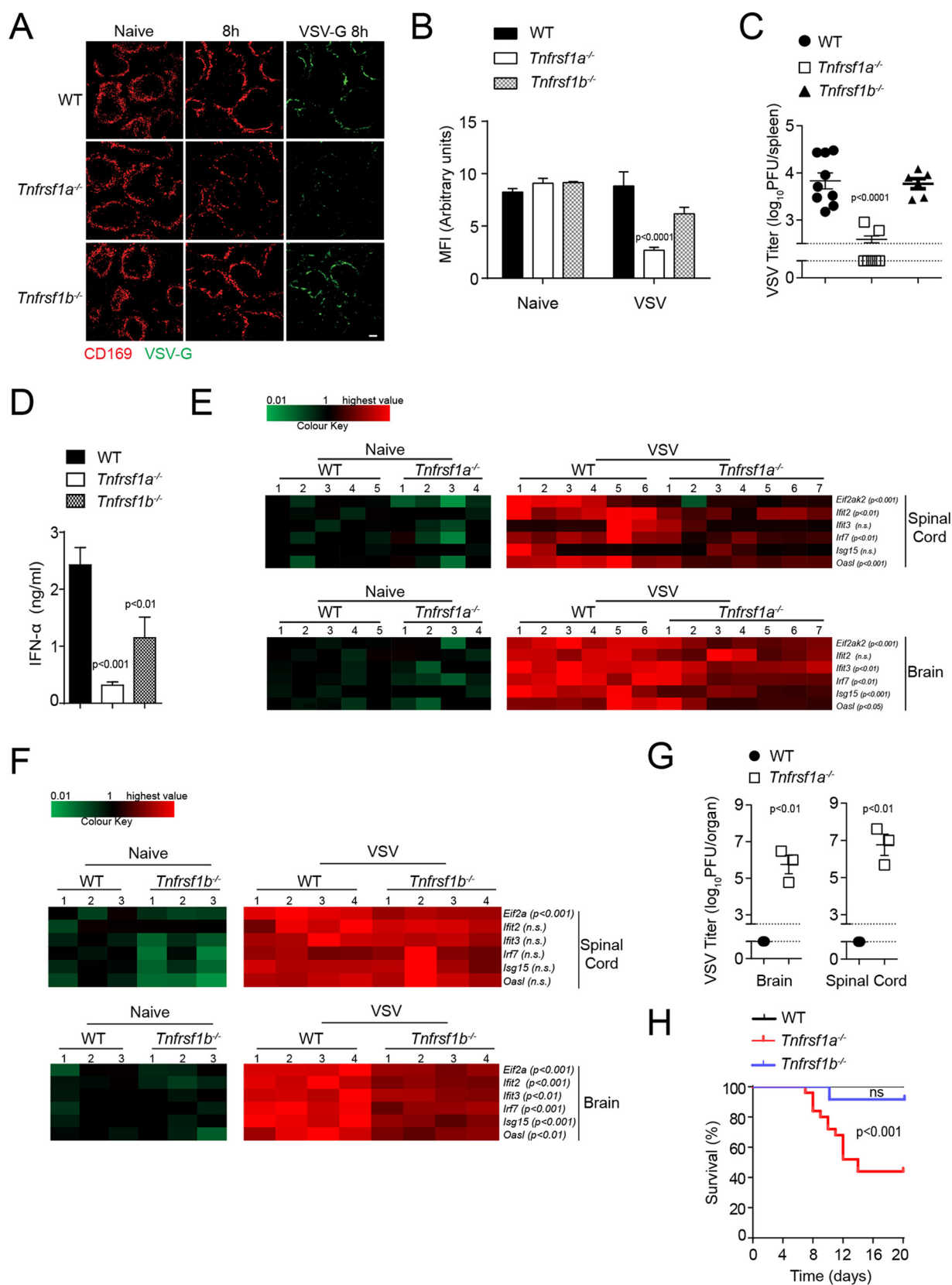


FIG 3 VSV replication is sustained via TNFR1 on CD169⁺ cells. (A) Spleen tissue sections from WT, *Tnfrsf1a*^{-/-} (TNFR1), and *Tnfrsf1b*^{-/-} (TNFR2) mice were stained with anti-CD169 and VSV-G antibodies 8 h after infection with 2×10^8 PFU of VSV (one representative result out of 6 mice is shown; scale bar = 100 μm). (B) MFI of CD169 was quantified across spleen sections from WT, *Tnfrsf1a*^{-/-}, and *Tnfrsf1b*^{-/-} infected mice, using ImageJ (1 to 3 images per spleen from 3 or 4 mice were analyzed). (C to G) WT, *Tnfrsf1a*^{-/-}, and *Tnfrsf1b*^{-/-} mice were infected with 10^5 PFU (Continued on next page)

The NF- κ B regulator MALT1 promotes canonical NF- κ B expression, VSV replication in CD169⁺ cells, and immune activation during viral infection. TNF can induce NF- κ B activation via TNFR1 and can promote the expression of genes driving survival and of proinflammatory cytokines (47). Furthermore, TNF is known to promote IFN-I production (48). Consistently, RelA expression was increased in the marginal zone of spleen tissue after VSV infection (Fig. 6A). We quantified cytoplasmic and nuclear expression of RelA in CD169⁺ cells. The nuclear presence of RelA in CD169⁺ cells was higher in VSV-infected mice than in naive controls (Fig. 6B). We wondered whether nuclear RelA protein expression was dependent on TNF. As expected, compared with WT control mice, VSV-infected mice exhibited reduced expression of RelA in the nuclear compartments of CD169⁺ cells in the absence of TNF (Fig. 6C). Notably, the presence of RelA was reduced in TNFR1-deficient mice, but we observed no difference in RelA expression between TNFR2-deficient mice and corresponding control mice (Fig. 6D and E). It has been reported that one of the major regulators of RelA signaling is RelB, which acts through sequestration of RelA in the cytoplasm and competitive binding of DNA (49). It has also been reported that the paracaspase MALT1 can promote canonical NF- κ B signaling by cleaving RelB (50, 51). Hence, we stained spleen sections of *Malt1*^{+/-} and *Malt1*^{-/-} mice for RelB. Ablation of MALT1 resulted in increased levels of RelB in CD169⁺ cells in the marginal zone of the spleen (Fig. 7A and B). In turn, nuclear RelA levels were lower in CD169⁺ cells in *Malt1*^{-/-} spleen tissue than in control tissue (Fig. 7C). Consistently, mouse embryonic fibroblasts (MEFs) derived from *Malt1*^{-/-} mice showed reduced translocation of p65 into the nucleus after stimulation with TNF but higher expression of RelB in the nucleus (Fig. 7D and E). These findings indicate that MALT1 destabilizes RelB in marginal-zone macrophages to promote canonical NF- κ B signaling. The presence of CD169⁺ cells in spleen tissue was not affected by *Malt1* before or after infection with VSV (Fig. 8A). However, the expression of VSV-G was lower in *Malt1*^{-/-} mice than in control mice (Fig. 8B and C). Consistently, the numbers of infectious VSV particles were lower in spleen tissue harvested from *Malt1*^{-/-} mice than in spleen tissue from control mice (Fig. 8D). Hence, serum IFN-I concentrations after VSV infection were lower in MALT1-deficient mice than in control mice (Fig. 8E). A previous report suggested that MALT1 is not required for RIG-I activation (52). Consistently, when we injected poly(I:C) into *Malt1*^{+/-} and *Malt1*^{-/-} mice, we found similar serum IFN-I levels in both groups (Fig. 8F). Hence, we concluded that defective IFN-I production during VSV infection was caused by reduced VSV replication early during infection. Consequently, MALT1-deficient mice succumbed to the infection, in sharp contrast to control animals (Fig. 8G).

Taken together, these findings indicate that absence of MALT1 results in reduced canonical NF- κ B signaling in response to VSV infection. *Malt1*-deficient mice exhibit reduced VSV replication and immune activation.

DISCUSSION

In this study, we found that TNF plays a crucial role in the maintenance of CD169⁺ cells early after infection with VSV. Consequently, TNF-, TNFR1-, and MALT1-deficient animals exhibited reduced immune activation and limited IFN-I production, which consequently led to severe VSV infection.

The role of TNF during viral infection is controversial and not sufficiently under-

FIG 3 Legend (Continued)

VSV. (C) Viral titers were measured in spleen tissue 8 h after infection in WT, *Tnfrsf1a*^{-/-}, and *Tnfrsf1b*^{-/-} mice (*n* = 6 to 9). The gap and dotted lines represent the detection limit of the virus plaque assay. (D) IFN- α concentrations were determined in the sera of WT, *Tnfrsf1a*^{-/-}, and *Tnfrsf1b*^{-/-} mice 24 h after infection with VSV (*n* = 6 to 9). (E) WT and *Tnfrsf1a*^{-/-} mice were infected with 10⁵ PFU VSV. RNA expression levels of the indicated genes were determined in brains and spinal cords 24 h after infection (*n* = 4 to 7). The highest relative expression values (brain/spinal cord) were as follows: *Eif2ak2*, 13.72/7.98; *Ilt2*, 5.41/6.13; *Ilt3*, 35.99/34.15; *Irf7*, 68.80/54.55; *Isg15*, 42.54/51.23; *Oas1*, 70.43/84.94. (F) WT and *Tnfrsf1b*^{-/-} mice were infected with 10⁵ PFU VSV. RNA expression levels of the indicated genes in brains and spinal cords were determined 24 h after infection (*n* = 3 or 4). The highest relative expression values (brain/spinal cord) were as follows: *Eif2ak2*, 29.84/18.21; *Ilt2*, 7.99/10.24; *Ilt3*, 41.05/51.25; *Irf7*, 166.79/88.58; *Isg15*, 29.78/52.99; *Oas1*, 75.60/114.39. (G) Viral titers were measured in brain and spinal cord tissue of WT and *Tnfrsf1a*^{-/-} mice once *Tnfrsf1a*^{-/-} mice exhibited hind limb paralysis (*n* = 3). (H) Survival of WT, *Tnfrsf1a*^{-/-}, and *Tnfrsf1b*^{-/-} mice was monitored over time after infection with VSV (*n* = 15 to 24). The error bars indicate SEM.

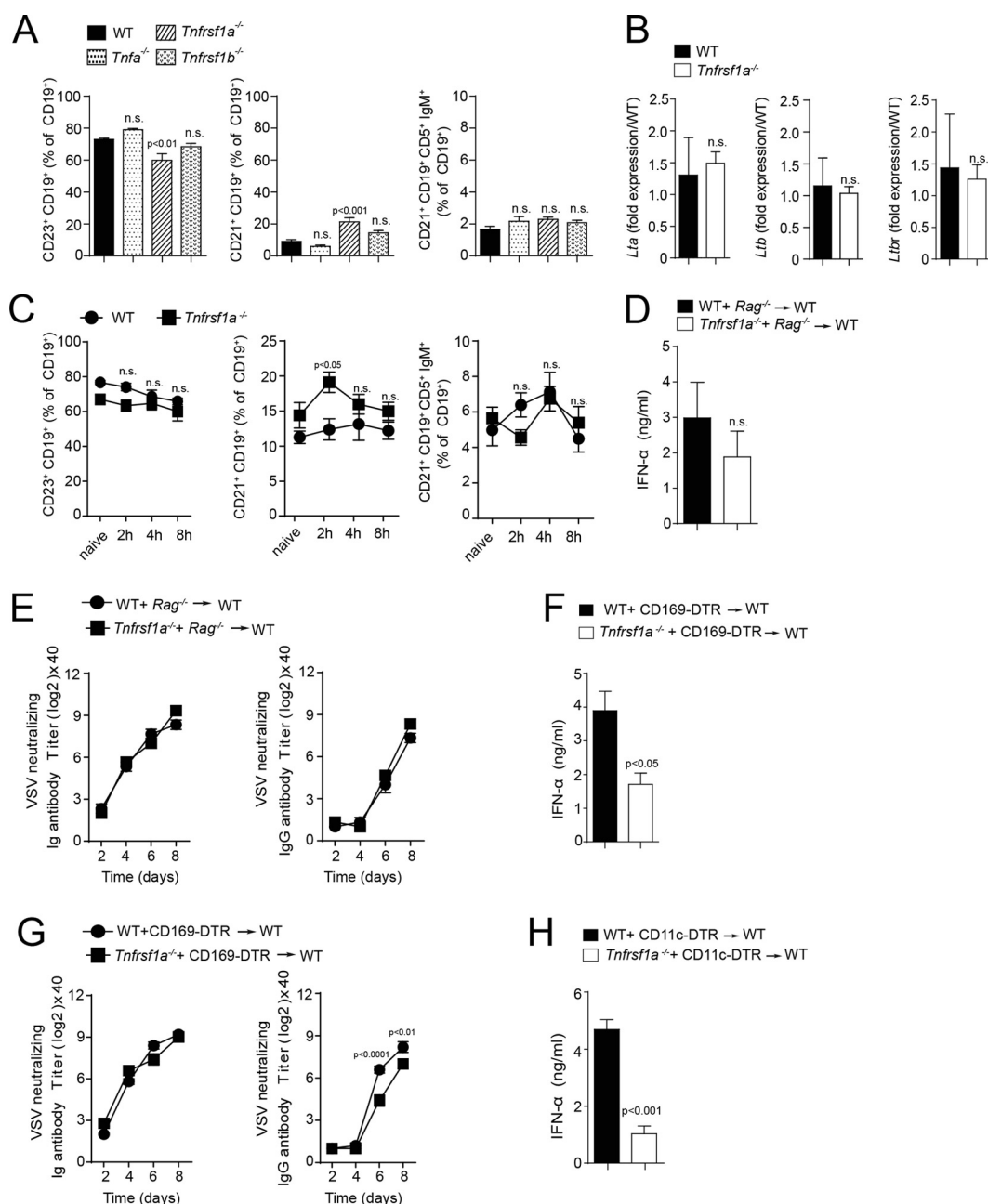


FIG 4 TNFR1 on CD169⁺ cells is essential for early IFN-I response. (A) Follicular B cells (CD19⁺ CD23⁺) (FB), marginal-zone B cells (CD19⁺ CD21⁺ CD23⁻) (MZB), and regulatory B cells (CD19⁺ CD21⁺ CD5⁺ IgM⁺) (RB) were analyzed in naive WT and *Tnfa*^{-/-}, *Tnfrsf1a*^{-/-}, and *Tnfrsf1b*^{-/-} mice ($n = 6$). (B) Lymphotoxin α (*Lta*), *Lt β* , and lymphotoxin β receptor (*Ltbr*) gene expression was determined in spleen tissue from WT and *Tnfrsf1a*^{-/-} mice by RT-PCR ($n = 3$). (C) Splenic B-cell populations (FB, MZB, and RB) were analyzed after infection with 2×10^8 PFU of VSV in WT and *Tnfrsf1a*^{-/-} mice at the indicated time points ($n = 5$). (D) IFN- α concentrations were determined 24 h after infection with 10^5 PFU VSV in the sera of lethally irradiated mice reconstituted with either WT-*Rag*^{-/-} or *Tnfrsf1a*^{-/-}-*Rag*^{-/-} bone marrow at a ratio of 1:1 ($n = 4$). (E) Neutralizing total immunoglobulin (left) and IgG (right) antibody titers were determined in the sera of WT-*Rag*^{-/-} or *Tnfrsf1a*^{-/-}-*Rag*^{-/-} reconstituted animals ($n = 4$). (F to H) Lethally irradiated WT mice were reconstituted with BM from WT or *Tnfrsf1a*^{-/-} mice mixed with BM from CD169-DTR (F) and CD11c-DTR (H) mice at a 1:1 ratio. After 40 days, the mice were infected with 10^5 PFU of VSV. Before infection, the mice were treated with 2 doses of 100 ng DT via intraperitoneal injection. (F) IFN- α concentrations were determined 24 h after infection in the sera of WT-CD169-DTR and *Tnfrsf1a*^{-/-}-CD169-DTR reconstituted animals ($n = 4$ or 5). (G) Neutralizing total immunoglobulin (left) and IgG (right) antibody titers were determined in the sera of WT-CD169-DTR and *Tnfrsf1a*^{-/-}-CD169-DTR reconstituted animals after infection with 10^5 PFU VSV at the indicated time points ($n = 4$). (H) IFN- α concentrations were determined 24 h after infection in the sera of WT-CD11c-DTR and *Tnfrsf1a*^{-/-}-CD11c-DTR reconstituted mice ($n = 4$ or 5). The error bars indicate SEM.

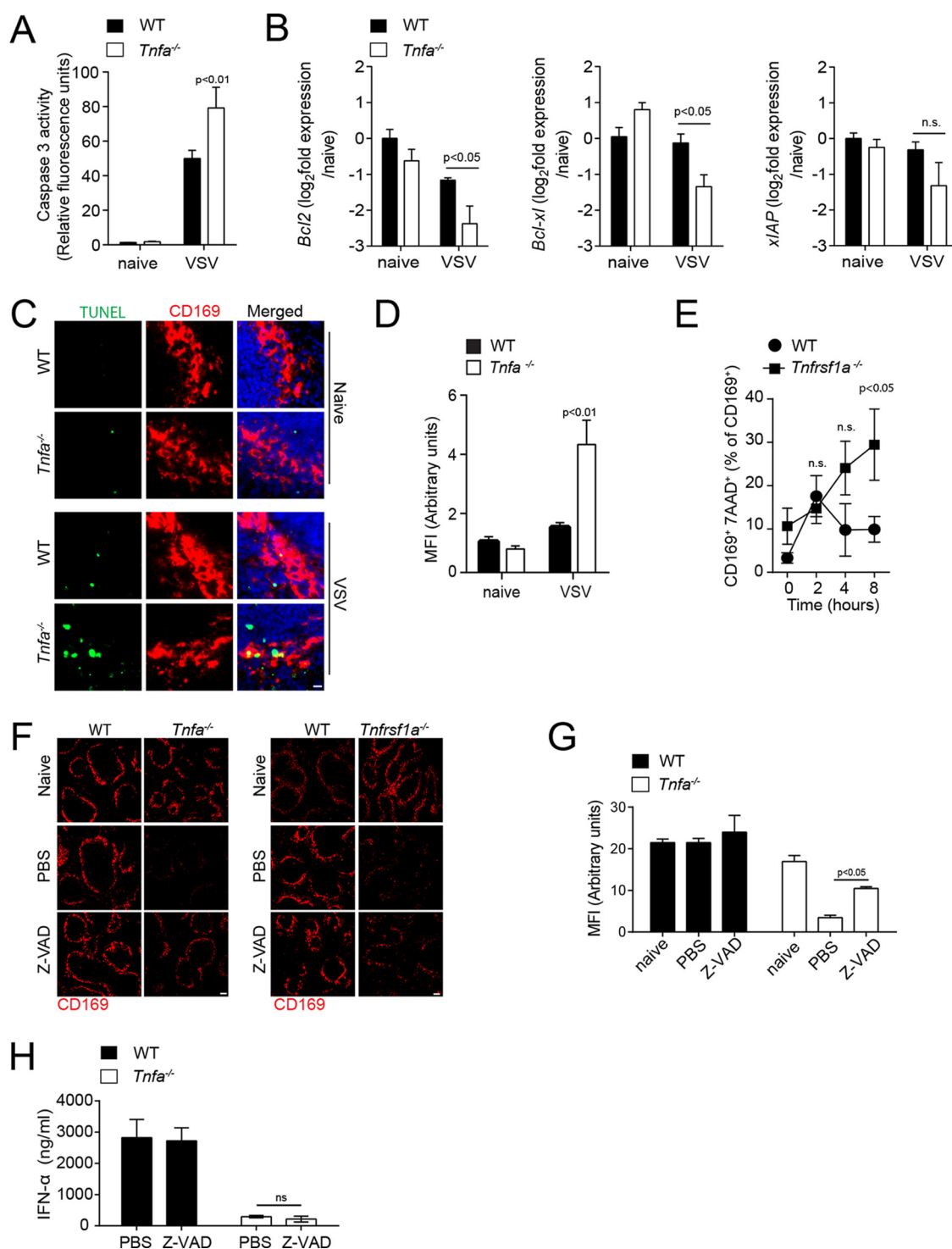


FIG 5 Tumor necrosis factor mediates survival of CD169⁺ cells via TNFR1. (A to E) Mice were infected with 2×10^8 PFU VSV. (A) Caspase 3 activity was determined in spleen tissue harvested from WT and *Tnfa*^{-/-} mice 6 h after infection with 2×10^8 PFU VSV ($n = 4$ to 7). (B) *Bcl2*, *Bclxl*, and *Xiap* RNA expression was determined in spleen tissue from WT and *Tnfrsf1a*^{-/-} mice 8 h after infection ($n = 3$). (C) Tissue sections from WT and *Tnfa*^{-/-} mice were TUNEL stained 5 h after infection (one result representative of 3 or 4 mice is shown; scale bar = 10 μ m). (D) MFI of TUNEL quantified across spleen sections from naive and VSV-infected WT and *Tnfa*^{-/-} mice using ImageJ (1 or 2 images per spleen from 3 or 4 mice were analyzed). (E) At the indicated time points, the proportions of 7AAD⁺ cells among CD11b⁺ CD169⁺ cells were determined ($n = 5$) in WT and *Tnfrsf1a*^{-/-} mice. (F) WT, *Tnfa*^{-/-}, and *Tnfrsf1a*^{-/-} mice were treated with Z-VAD and infected with 2×10^8 PFU VSV. Spleen tissue sections were stained with anti-CD169 antibodies 8 h after infection (one result representative of 3 or 4 mice is shown; scale bar = 100 μ m). (G) MFI of CD169 quantified across spleen sections from naive and VSV-infected WT and *Tnfa*^{-/-} mice treated with Z-VAD, using ImageJ (1 to 3 images per spleen from 3 or 4 mice were analyzed). (H) IFN- α concentrations determined 24 h after infection in the sera of Z-VAD-treated WT and *Tnfa*^{-/-} mice after infection with 10^5 PFU of VSV ($n = 3$). The error bars indicate SEM.

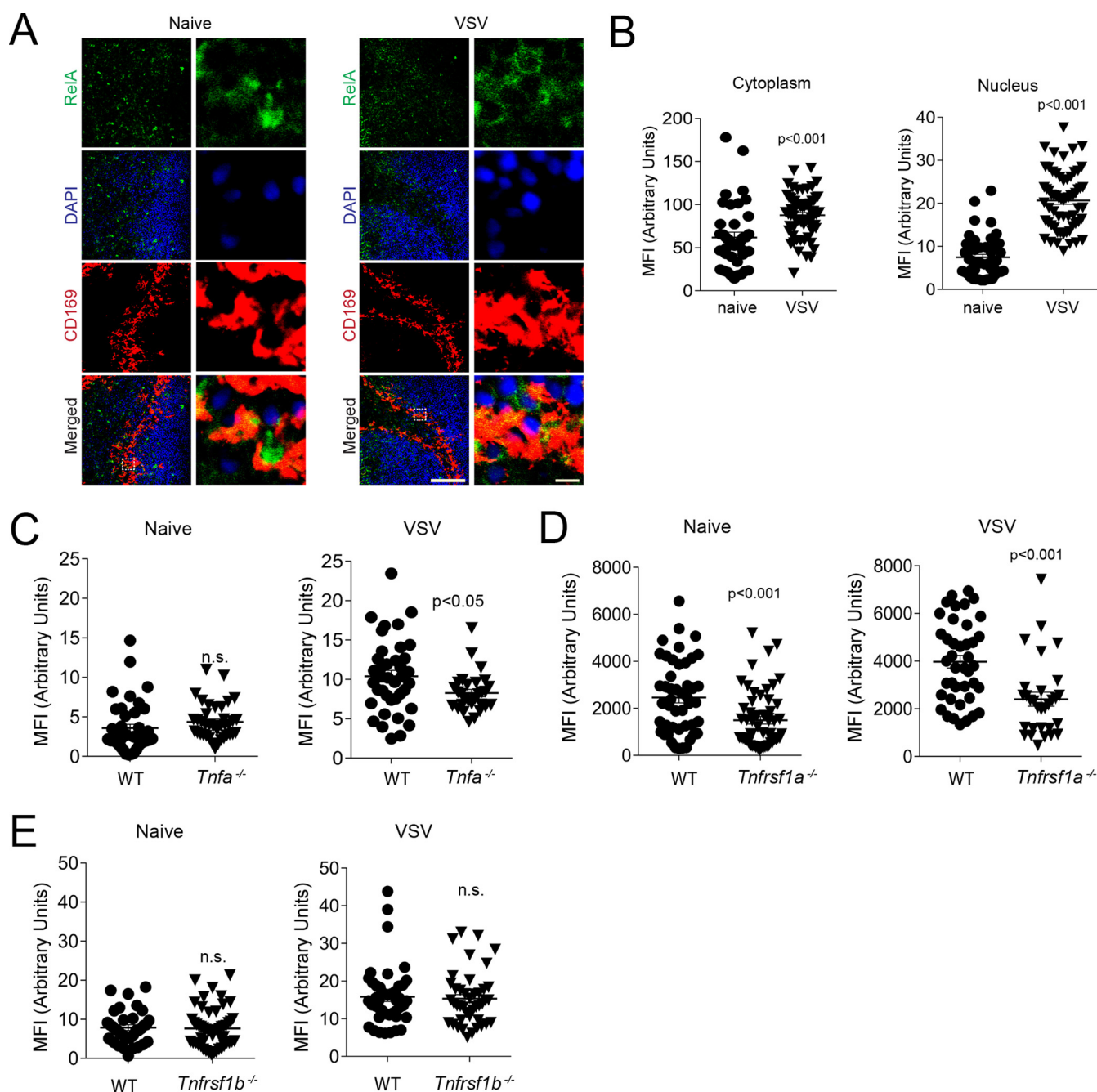


FIG 6 VSV infection leads to TNFR1-dependent canonical NF- κ B activation in splenic CD169⁺ cells. (A to D) Sections of snap-frozen spleen tissue were harvested 4 h after infection with 2×10^8 PFU VSV. (A) The sections were stained for RelA before and after infection (one representative result out of 3 is shown; scale bar = 100 μ m). Enlarged images of the boxed areas in the merged images on the left side are shown on the right (scale bar = 5 μ m). (B) MFI of cytoplasmic and respective nuclear RelA quantified in CD169⁺ cells from WT mice before and after VSV infection to evaluate nuclear translocation of RelA ($n = 48$ to 63). (C to E) Spleen sections from WT and $Tnfa^{-/-}$ (C), $Tnfrsf1a^{-/-}$ (D), and $Tnfrsf1b^{-/-}$ (E) mice were stained with anti-RelA antibodies 4 h after infection with 2×10^8 PFU VSV. The MFI of RelA in the nuclei of CD169⁺ cells was determined with ImageJ software ($n = 35$ to 57). The error bars indicate SEM.

stood. Although reports describe activating polymorphisms in TNF, which are associated with the establishment of a chronic viral infection (53), other reports state that the same mutations are protective against chronic hepatitis B virus (HBV) infection (54). *In vitro*, TNF can propagate the replication of hepatitis C virus (HCV) (55), although HCV increases the incidence of TNF-induced apoptosis (56). On the other hand, TNF strongly inhibits influenza virus replication in porcine lung epithelial cells (57). Consistently, the attenuation of TNF signaling in a murine T-cell-independent model of HBV infection

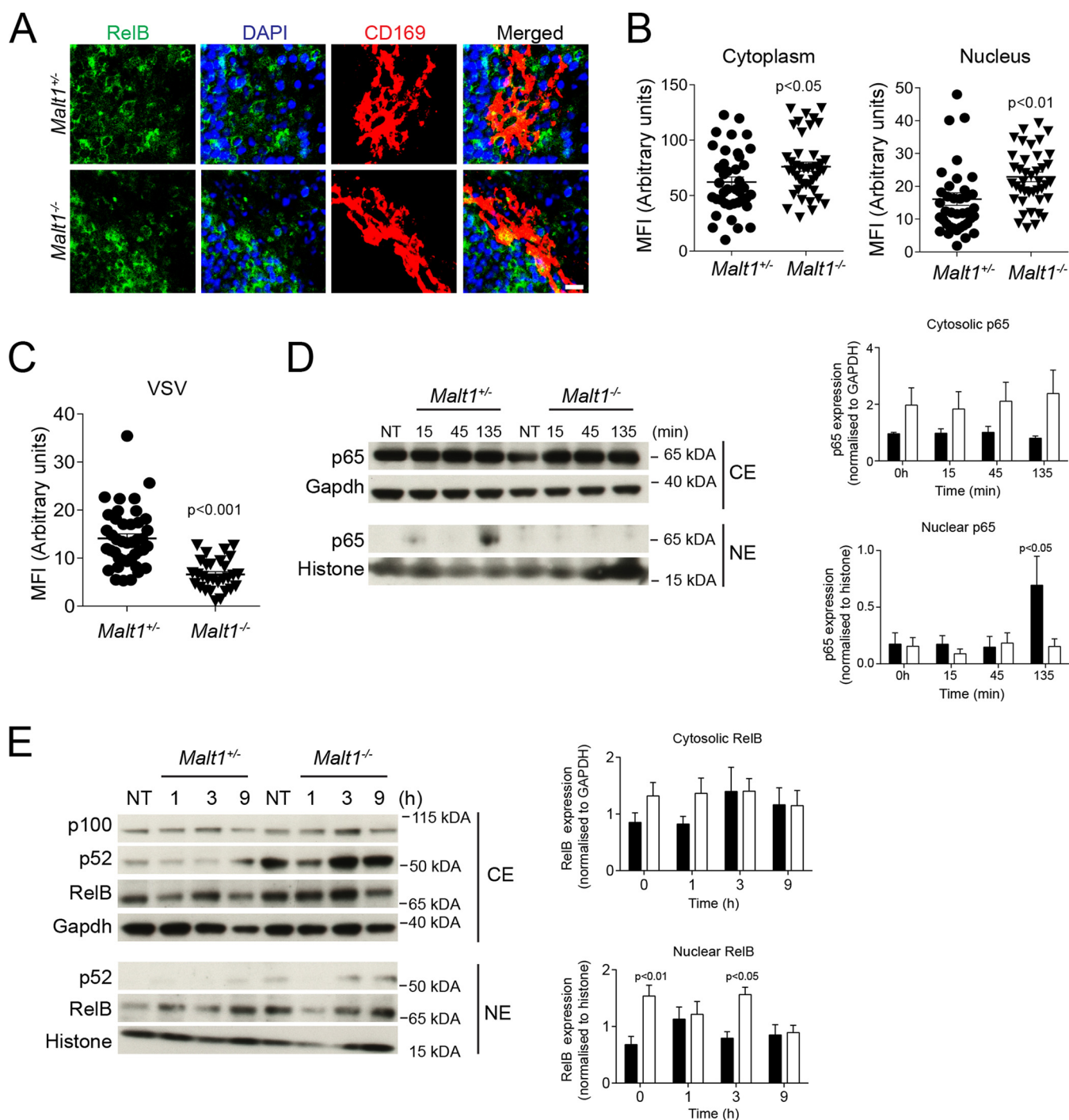


FIG 7 MALT1 regulates nuclear RelA expression after infection with vesicular stomatitis virus. (A) Sections from snap-frozen spleen tissue harvested from naive *Malt1*^{+/+} and *Malt1*^{-/-} mice were stained with anti-RelB antibodies (one representative result out of 3 is shown; scale bar = 10 μ m). (B) MFI of cytoplasmic and nuclear RelB was quantified in CD169⁺ cells using ImageJ ($n = 39$ to 42). (C) Sections of snap-frozen spleen tissue from *Malt1*^{+/+} and *Malt1*^{-/-} mice were stained with anti-RelA antibodies 4 h after infection with 2×10^8 PFU VSV. The MFI in the nuclei of CD169⁺ cells was quantified ($n = 29$ to 41). (D and E) *Malt1*^{+/+} and *Malt1*^{-/-} MEFs were stimulated with 100 ng/ml recombinant mouse tumor necrosis factor (rmTNF) at the indicated time points. Cytosolic extracts (CE) and nuclear extracts (NE) were harvested and probed for p65. Densitometry analysis of p65 and RelB was performed on the Western blot (WB) images from cytosolic and nuclear fractions at the indicated time points. Proteins were normalized to GAPDH or histone ($n = 4$). The error bars indicate SEM.

results in viral persistence (58). In turn, the application of second mitochondrion-derived activator of caspases (SMAC) mimetics enhances TNF signaling and is associated with increased clearance of HBV in this model system (59). During infection with VSV, the production of neutralizing antibodies is not defective in the absence of TNFR1 (32). Moreover, TNF can induce T-cell dysfunction and therefore promote chronic viral

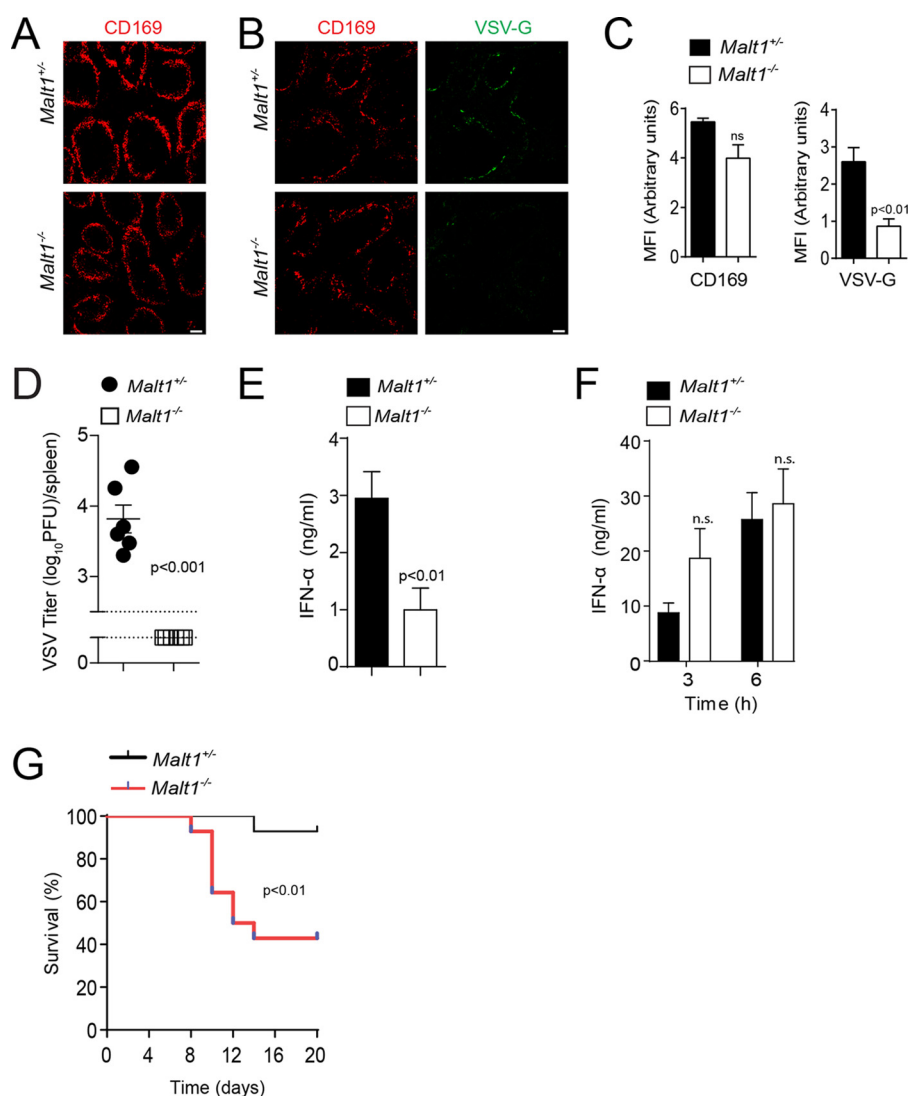


FIG 8 MALT1 promotes vesicular stomatitis virus replication in CD169⁺ cells and immune activation during viral infection. (A) Spleen sections from naive *Malt1*^{+/+} and *Malt1*^{-/-} mice were stained with anti-CD169 (one representative result out of 3 is shown; scale bar = 100 μm). (B) Sections of snap-frozen spleen tissue from *Malt1*^{+/+} and *Malt1*^{-/-} mice were analyzed 8 h after infection with 2 × 10⁸ PFU VSV and stained with anti-CD169 and anti-VSV-G (one representative result out of 3 is shown; scale bar = 100 μm). (C) MFI of CD169 and VSV-G was quantified across spleen sections from VSV-infected *Malt1*^{+/+} and *Malt1*^{-/-} mice using ImageJ (*n* = 4). (D and E) Mice were infected with 10⁵ PFU VSV. (D) Viral titers were measured in spleen tissue of *Malt1*^{+/+} and *Malt1*^{-/-} mice 8 h after infection (*n* = 6). (E) IFN-α concentrations were determined in the sera of *Malt1*^{+/+} and *Malt1*^{-/-} mice 24 h after infection (*n* = 6). (F) IFN-α concentrations were determined in the sera of *Malt1*^{+/+} and *Malt1*^{-/-} mice injected with 200 μg poly(I:C) at the indicated time points (*n* = 3 or 4). (G) Survival of *Malt1*^{+/+} and *Malt1*^{-/-} animals was monitored for 20 days after infection (*n* = 13 to 14). The error bars indicate SEM.

infection (60). Our finding that TNF is crucial for the maintenance of CD169⁺ cells in spleen tissue may be important for infections with lower doses of virus, because allowing viral replication in CD169⁺ cells is particularly important for protective adaptive immunity (9, 13). This may be crucial for the maintenance of CD169⁺ cells in spleen tissue during vaccination with attenuated virus strains or VSV vector-based vaccines (25). These findings may not be specific only for splenic CD169⁺ cells, since intranasal infection with recombinant TNF overexpressing rabies virus (RV) reduced the RV load and mortality (61).

Viral replication in CD169⁺ cells, which is promoted by TNF, contributes to improved antigen presentation. CD169⁺ cells in the marginal zone are in close contact with

pathogens and are ideally situated to induce an immune response (62). Furthermore, CD169⁺ cells have been shown not only to present antigens to B cells in the lymph nodes, but also to prime T cells (11, 63). Moreover, CD169⁺ cells are important for virus-mediated IFN-I production, which prevents severe CNS infection in mice (64). Our findings show that TNF promotes maintenance of CD169⁺ cells and IFN-I production following VSV infection. Furthermore, our findings show that the translocation of RelA to the nuclei of CD169⁺ cells after VSV infection is dependent on TNF. It has been postulated that canonical NF- κ B can contribute to the production of IFN- α (65, 66). However, RelA-deficient and p50-deficient MEFs can produce IFN- α after viral infection, whereas only early IFN-I transcription is reduced (67, 68). Furthermore, RelA-deficient plasmacytoid dendritic cells (pDCs) exhibited reduced IFN production after exposure to Sendai virus (69). Our findings indicate that canonical NF- κ B activation can also promote early viral replication and consequently contribute to the production of IFN-I. Consistently, noncanonical NF- κ B, which can inhibit canonical NF- κ B signaling, is a potent inhibitor of IFN-I production (70). Hence, the paracaspase MALT1, which can cleave RelB and consequently promote canonical NF- κ B signaling (50, 51), is necessary for the sufficient propagation of VSV replication and IFN-I production.

Taken together, we have found that TNF-TNFR1 signaling is crucial for protecting CD169⁺ cells and their function in innate immune activation during VSV infection.

MATERIALS AND METHODS

Mice, viruses, and virus titration. *Tnfa*^{-/-}, *Tnfrsf1b*^{-/-}, *CD8*^{-/-}, and *Rag1*^{-/-} mice were purchased from Jackson Laboratories (United States). *Tnfrsf1a*^{-/-} mice have been previously described (34). *Malt1*^{-/-}, *CD169*^{-/-}, *CD169-DTR*, and *CD11c-DTR* mice have also been previously described (71–74). All the mice were maintained on a C57BL/6 genetic background. VSV Indiana serotype (Mudd-Summers strain) was originally obtained from D. Kolakofsky (University of Geneva, Geneva, Switzerland). VSV was propagated and titrated as previously described (13). Mice were infected with VSV via tail vein injection. In survival experiments, mice exhibiting symptoms of hind leg paralysis were considered “severe,” taken out of the experiment, and counted as dead. Blood was collected at the indicated time points after infection. VSV neutralizing antibody titers were measured by plaque reduction neutralization test (PRNT) as previously described (9, 13). Briefly, serum samples were diluted 1:40 and incubated at 56°C for 30 min. To evaluate immunoglobulin G (IgG), the serum was pretreated with 0.1 M β -mercaptoethanol. Serial 2-fold dilutions were performed for 12 steps, and the serum was incubated with 5,000 PFU of VSV. The virus and serum mixture was incubated on a Vero cell monolayer. The plates were stained with crystal violet after 24 h. To inhibit caspase activity *in vivo*, we administered three doses (2 μ g/g of body weight each) of Z-VAD (Abcam, Cambridge, United Kingdom) (75, 76). For chimera experiments, mice were lethally irradiated with 10.2 Gy. After 24 h, mixed bone marrow from WT or *Tnfrsf1a*^{-/-} and *CD169-DTR*, *CD11c-DTR*, and *Rag1*^{-/-} mice was transplanted into the irradiated mice as indicated. All mice were maintained under specific-pathogen-free conditions under the authorization of the Landesamt für Natur, Umwelt und Verbraucherschutz of North Rhine-Westphalia (LANUV NRW) in accordance with the German laws for animal protection.

Depletion of cells. To deplete macrophages, 200 μ l clodronate liposomes was injected intravenously, and 24 h later, the mice were infected with VSV. Liposomes containing phosphate-buffered saline (PBS; PBS liposomes) were used as a control. Clodronate and PBS liposomes were provided by Nico van Rooijen (Vrije University Medical Center, Netherlands) and used as previously described (41, 42). CD169- and CD11c-expressing cells in *CD169-DTR* and *CD11c-DTR* mice were depleted by injecting 2 doses of 100 ng DT (Sigma) 1 day before and on the day of infection.

Histology and ELISA. Histological analysis of snap-frozen tissue was performed as previously described (9). Briefly, snap-frozen tissue sections were cut at 7- μ m thickness, air dried, and fixed with acetone for 10 min. The sections were blocked with 2% fetal calf serum in phosphate-buffered saline (PBS) for 1 h and stained with anti-CD169 (final concentration, 4 μ g/ml; Acris, Germany; clone MOMA-1), anti-VSV-G (final concentration, 1 μ g/ml; produced in house; clone Vi10), anti-RelA (final concentration, 1 μ g/ml; Santa Cruz Biotechnology, USA), anti-F4/80 (final concentration, 2 μ g/ml; eBioscience; clone BM8), and anti-RelB (final concentration, 1 μ g/ml; Cell Signaling, USA; polyclonal) for 1 h. Then, the sections were washed with PBS containing 0.05% Tween 20 (Sigma). The secondary antibodies, phycoerythrin (PE) streptavidin (final concentration, 1 μ g/ml; eBioscience), anti-rabbit fluorescein isothiocyanate (FITC) (final concentration, 1 μ g/ml; Thermo Fisher), and anti-goat FITC (final concentration, 1 μ g/ml; Santa Cruz Biotechnology, USA), were incubated for 1 h. Then, the sections were washed with PBS containing 0.05% Tween 20 (Sigma) and mounted using fluorescence mounting medium (Dako). A caspase 3 activity assay was performed with a fluorescence assay (Cell Signaling) according to the manufacturer's instructions. TUNEL staining was performed on formalin-fixed spleen sections according to the manufacturer's instructions (Thermo Scientific, USA). Images were obtained with an LSM510 confocal microscope and an Axio Observer Z1 fluorescence microscope (Zeiss, Germany). Analysis of the fluorescence images was performed with ImageJ software. IFN- α and IFN- β (PBL Biosciences, New Jersey,

USA) concentrations were determined using an enzyme-linked immunosorbent assay (ELISA) according to the manufacturers' instructions.

Reverse transcription (RT)-PCR analyses. RNA purification (Qiagen RNeasy kit or TRIzol) was performed according to the manufacturer's instructions. Gene expression of *Bcl2*, *Bcl-xl*, *Xiap*, *Lta*, *Ltb*, *Ifit1*, *Ifit2*, *Ifit3*, *Irf7*, *Isg15*, *Oas1*, and *Tnfa* was performed using 6-carboxyfluorescein (FAM) and VIC probes (Applied Biosystems) and an iTAQ one-step PCR kit (Bio-Rad). For analysis, the expression levels of all the target genes were normalized to β -actin/GAPDH (glyceraldehyde-3-phosphate dehydrogenase) expression (ΔC_T). Gene expression values were then calculated based on the $\Delta\Delta C_T$ method, using naive WT mice as a control to which all other samples were compared. Relative quantities (RQ) were determined using the following equation: $RQ = 2^{-\Delta\Delta C_T}$.

Immunoblotting. *Malt1*^{+/-} and *Malt1*^{-/-} MEFs were obtained from Jürgen Ruland (Technische Universität Munich, Munich, Germany). *Malt1*^{+/-} and *Malt1*^{-/-} MEFs were stimulated with 100 ng/ml murine soluble TNF (mTNF) (R&D Systems). Cytoplasmic and nuclear extracts were prepared using a nuclear protein extraction kit according to the manufacturer's instructions (Active Motif, Belgium). Immunoblots were probed with primary anti-p65 (Santa Cruz Biotechnology), anti-RelB (Cell Signaling), and anti-p100/p52 (Cell Signaling).

Flow cytometry. For intracellular-cytokine staining, single-cell suspended splenocytes were incubated with brefeldin A (eBioscience), followed by an additional 5 h of incubation at 37°C. After surface staining with anti-CD3, anti-CD8, anti-CD11b, anti-CD11c, anti-CD19, anti-CD115, anti-F4/80, anti-Ly6C, anti-Ly6G, anti-MHC-II, and anti-NK1.1 antibodies (all from eBioscience), the cells were fixed with 2% formalin, permeabilized with 0.1% saponin, and stained with anti-TNF antibodies (eBioscience) for 30 min at 4°C. B-cell subsets were detected in single-cell suspensions of splenocytes with anti-CD5, anti-CD19, anti-CD21, anti-CD23, and anti-IgM antibodies (all from eBioscience). BD Calibrite (BD Biosciences, USA) beads were added to the samples before acquisition with a BD LSRFortessa.

Statistical analyses. Data are represented with standard errors of the mean (SEM). Statistically significant differences between two groups were determined with Student's *t* test. Statistically significant differences between several groups were determined by one-way analysis of variance (ANOVA) with additional Bonferroni or Dunnett *post hoc* tests. Statistically significant differences between groups in experiments involving more than one time point were determined with two-way ANOVA (repeated measurements).

ACKNOWLEDGMENTS

We thank Flo Witte for valuable comments on the manuscript.

This study was supported by the Alexander von Humboldt Foundation (SKA2010), the German Research Council (SFB974, LA2558/3-1, LA2558/5-1, GRK1949, and TRR60), Jürgen Manchot Graduate School MOI II, and the NIH tetramer facility. D.B. is funded by the ATTRACT Programme (A14/BM/7632103/DBRRIL) and a CORE grant (C15/BM/10355103) from the National Research Fund Luxembourg (FNR). J.R. is funded by the DFG (SFB 1054/B01) and the ERC (FP7; grant agreement no. 322865).

REFERENCES

- McNab F, Mayer-Barber K, Sher A, Wack A, O'Garra A. 2015. Type I interferons in infectious disease. *Nat Rev Immunol* 15:87–103. <https://doi.org/10.1038/nri3787>.
- Chavez-Galan L, Olleros ML, Vesin D, Garcia I. 2015. Much more than M1 and M2 macrophages, There are also CD169(+) and TCR(+) macrophages. *Front Immunol* 6:263. <https://doi.org/10.3389/fimmu.2015.00263>.
- Mebius RE, Kraal G. 2005. Structure and function of the spleen. *Nat Rev Immunol* 5:606–616. <https://doi.org/10.1038/nri1669>.
- Snook T. 1964. Studies on the perifollicular region of the rat's spleen. *Anat Rec* 148:149–159. <https://doi.org/10.1002/ar.1091480205>.
- Crocker PR, Gordon S. 1986. Properties and distribution of a lectin-like hemagglutinin differentially expressed by murine stromal tissue macrophages. *J Exp Med* 164:1862–1875. <https://doi.org/10.1084/jem.164.6.1862>.
- Kraal G, Janse M. 1986. Marginal metallophilic cells of the mouse spleen identified by a monoclonal antibody. *Immunology* 58:665–669.
- Oetke C, Kraal G, Crocker PR. 2006. The antigen recognized by MOMA-1 is sialoadhesin. *Immunol Lett* 106:96–98. <https://doi.org/10.1016/j.imlet.2006.04.004>.
- Gupta P, Lai SM, Sheng J, Tetlak P, Balachander A, Claser C, Renia L, Karjalainen K, Ruedl C. 2016. Tissue-resident CD169(+) macrophages form a crucial front line against plasmodium infection. *Cell Rep* 16:1749–1761. <https://doi.org/10.1016/j.celrep.2016.07.010>.
- Honke N, Shaabani N, Cadeddu G, Sorg UR, Zhang DE, Trilling M, Klingel K, Sauter M, Kandolf R, Gailus N, van Rooijen N, Burkart C, Baldus SE, Grusdat M, Lohning M, Hengel H, Pfeffer K, Tanaka M, Haussinger D, Recher M, Lang PA, Lang KS. 2012. Enforced viral replication activates adaptive immunity and is essential for the control of a cytopathic virus. *Nat Immunol* 13:51–57. <https://doi.org/10.1038/ni.2169>.
- Iannaccone M, Moseman EA, Tonti E, Bosurgi L, Junt T, Henrickson SE, Whelan SP, Guidotti LG, von Andrian UH. 2010. Subcapsular sinus macrophages prevent CNS invasion on peripheral infection with a neurotropic virus. *Nature* 465:1079–1083. <https://doi.org/10.1038/nature09118>.
- Junt T, Moseman EA, Iannaccone M, Massberg S, Lang PA, Boes M, Fink K, Henrickson SE, Shayakhmetov DM, Di Paolo NC, van Rooijen N, Mempel TR, Whelan SP, von Andrian UH. 2007. Subcapsular sinus macrophages in lymph nodes clear lymph-borne viruses and present them to antiviral B cells. *Nature* 450:110–114. <https://doi.org/10.1038/nature06287>.
- Tumanov A, Kuprash D, Lagarkova M, Grivnenkov S, Abe K, Shakhov A, Drutskaya L, Stewart C, Chervonsky A, Nedospasov S. 2002. Distinct role of surface lymphotoxin expressed by B cells in the organization of secondary lymphoid tissues. *Immunity* 17:239–250. [https://doi.org/10.1016/S1074-7613\(02\)00397-7](https://doi.org/10.1016/S1074-7613(02)00397-7).
- Xu HC, Huang J, Khairnar V, Duhan V, Pandya AA, Grusdat M, Shinde P, McIlwain DR, Maney SK, Gommerman J, Lohning M, Ohashi PS, Mak TW, Pieper K, Sic H, Speletas M, Eibel H, Ware CF, Tumanov AV, Kruglov AA, Nedospasov SA, Haussinger D, Recher M, Lang KS, Lang PA. 2015. Deficiency of the B cell-activating factor receptor results in limited CD169+ macrophage function during viral infection. *J Virol* 89:4748–4759. <https://doi.org/10.1128/JVI.02976-14>.
- Khairnar V, Duhan V, Maney SK, Honke N, Shaabani N, Pandya AA, Seifert M, Pozdeev V, Xu HC, Sharma P, Baldin F, Marquardsen F, Merches

- K, Lang E, Kirschning C, Westendorf AM, Haussinger D, Lang F, Dittmer U, Kuppers R, Recher M, Hardt C, Scheffrahn I, Beauchemin N, Gothert JR, Singer BB, Lang PA, Lang KS. 2015. CEACAM1 induces B-cell survival and is essential for protective antiviral antibody production. *Nat Commun* 6:6217. <https://doi.org/10.1038/ncomms7217>.
15. Muller U, Steinhoff U, Reis LF, Hemmi S, Pavlovic J, Zinkernagel RM, Aguet M. 1994. Functional role of type I and type II interferons in antiviral defense. *Science* 264:1918–1921. <https://doi.org/10.1126/science.8009221>.
 16. Kawai T, Akira S. 2009. The roles of TLRs, RLRs and NLRs in pathogen recognition. *Int Immunol* 21:317–337. <https://doi.org/10.1093/intimm/dxp017>.
 17. Lichty BD, Power AT, Stojdl DF, Bell JC. 2004. Vesicular stomatitis virus: re-inventing the bullet. *Trends Mol Med* 10:210–216. <https://doi.org/10.1016/j.molmed.2004.03.003>.
 18. Hangartner L, Zinkernagel RM, Hangartner H. 2006. Antiviral antibody responses: the two extremes of a wide spectrum. *Nat Rev Immunol* 6:231–243. <https://doi.org/10.1038/nri1783>.
 19. Bi Z, Barna M, Komatsu T, Reiss CS. 1995. Vesicular stomatitis virus infection of the central nervous system activates both innate and acquired immunity. *J Virol* 69:6466–6472.
 20. Chauhan VS, Furr SR, Sterka DG, Jr, Nelson DA, Moerdyk-Schauwecker M, Marriott I, Gzdelishvili VZ. 2010. Vesicular stomatitis virus infects resident cells of the central nervous system and induces replication-dependent inflammatory responses. *Virology* 400:187–196. <https://doi.org/10.1016/j.virol.2010.01.025>.
 21. Christian AY, Barna M, Bi Z, Reiss CS. 1996. Host immune response to vesicular stomatitis virus infection of the central nervous system in C57BL/6 mice. *Viral Immunol* 9:195–205. <https://doi.org/10.1089/vim.1996.9.195>.
 22. Huneycutt BS, Bi Z, Aoki CJ, Reiss CS. 1993. Central neuropathogenesis of vesicular stomatitis virus infection of immunodeficient mice. *J Virol* 67:6698–6706.
 23. Fensterl V, Wetzel JL, Ramachandran S, Ogino T, Stohman SA, Bergmann CC, Diamond MS, Virgin HW, Sen GC. 2012. Interferon-induced Ifit2/ISG54 protects mice from lethal VSV neuropathogenesis. *PLoS Pathog* 8:e1002712. <https://doi.org/10.1371/journal.ppat.1002712>.
 24. Trottier MD, Jr, Palian BM, Reiss CS. 2005. VSV replication in neurons is inhibited by type I IFN at multiple stages of infection. *Virology* 333: 215–225. <https://doi.org/10.1016/j.virol.2005.01.009>.
 25. Jones SM, Feldmann H, Stroher U, Geisbert JB, Fernando L, Grolla A, Klenk HD, Sullivan NJ, Volchkov VE, Fritz EA, Daddario KM, Hensley LE, Jahrling PB, Geisbert TW. 2005. Live attenuated recombinant vaccine protects nonhuman primates against Ebola and Marburg viruses. *Nat Med* 11:786–790. <https://doi.org/10.1038/nm1258>.
 26. Pasparakis M, Kousteni S, Peschon J, Kollias G. 2000. Tumor necrosis factor and the p55TNF receptor are required for optimal development of the marginal sinus and for migration of follicular dendritic cell precursors into splenic follicles. *Cell Immunol* 201:33–41. <https://doi.org/10.1006/cimm.2000.1636>.
 27. Engwerda CR, Ato M, Cotterell SE, Mynott TL, Tschannerl A, Gorak-Stolinska PM, Kaye PM. 2002. A role for tumor necrosis factor- α in remodeling the splenic marginal zone during *Leishmania donovani* infection. *Am J Pathol* 161:429–437. [https://doi.org/10.1016/S0002-9440\(10\)64199-5](https://doi.org/10.1016/S0002-9440(10)64199-5).
 28. Calzascia T, Pellegrini M, Hall H, Sabbagh L, Ono N, Elford AR, Mak TW, Ohashi PS. 2007. TNF- α is critical for antitumor but not antiviral T cell immunity in mice. *J Clin Invest* 117:3833–3845.
 29. Wang T, Town T, Alexopoulou L, Anderson JF, Fikrig E, Flavell RA. 2004. Toll-like receptor 3 mediates West Nile virus entry into the brain causing lethal encephalitis. *Nat Med* 10:1366–1373. <https://doi.org/10.1038/nm1140>.
 30. Lundberg P, Welander PV, Edwards CK III, van Rooijen N, Cantin E. 2007. Tumor necrosis factor (TNF) protects resistant C57BL/6 mice against herpes simplex virus-induced encephalitis independently of signaling via TNF receptor 1 or 2. *J Virol* 81:1451–1460. <https://doi.org/10.1128/JVI.02243-06>.
 31. Vilela MC, Lima GK, Rodrigues DH, Lacerda-Queiroz N, Mansur DS, de Miranda AS, Rachid MA, Kroon EG, Vieira LQ, Campos MA, Teixeira MM, Teixeira AL. 2010. TNFR1 plays a critical role in the control of severe HSV-1 encephalitis. *Neurosci Lett* 479:58–62. <https://doi.org/10.1016/j.neulet.2010.05.028>.
 32. Fehr T, Bachmann MF, Bluethmann H, Kikutani H, Hangartner H, Zinkernagel RM. 1996. T-independent activation of B cells by vesicular stomatitis virus: no evidence for the need of a second signal. *Cell Immunol* 168:184–192. <https://doi.org/10.1006/cimm.1996.0065>.
 33. Rothe J, Lesslauer W, Lotscher H, Lang Y, Koebel P, Kontgen F, Althage A, Zinkernagel R, Steinmetz M, Bluethmann H. 1993. Mice lacking the tumour necrosis factor receptor 1 are resistant to TNF-mediated toxicity but highly susceptible to infection by *Listeria monocytogenes*. *Nature* 364:798–802. <https://doi.org/10.1038/364798a0>.
 34. Pfeffer K, Matsuyama T, Kundig TM, Wakeham A, Kishihara K, Shahinian A, Wiegmann K, Ohashi PS, Kronke M, Mak TW. 1993. Mice deficient for the 55 kd tumor necrosis factor receptor are resistant to endotoxic shock, yet succumb to *L. monocytogenes* infection. *Cell* 73:457–467.
 35. Botha T, Ryffel B. 2003. Reactivation of latent tuberculosis infection in TNF-deficient mice. *J Immunol* 171:3110–3118. <https://doi.org/10.4049/jimmunol.171.6.3110>.
 36. Wellmer A, Gerber J, Ragheb J, Zysk G, Kunst T, Smirnov A, Bruck W, Nau R. 2001. Effect of deficiency of tumor necrosis factor α or both of its receptors on *Streptococcus pneumoniae* central nervous system infection and peritonitis. *Infect Immun* 69:6881–6886. <https://doi.org/10.1128/IAI.69.11.6881-6886.2001>.
 37. Bartholdy C, Nansen A, Marker O, Thomsen AR. 1999. Soluble tumour necrosis factor (TNF)-receptor levels in serum as markers of anti-viral host reactivity. *Clin Exp Immunol* 116:299–306. <https://doi.org/10.1046/j.1365-2249.1999.00903.x>.
 38. Brandes M, Klauschen F, Kuchen S, Germain RN. 2013. A systems analysis identifies a feedforward inflammatory circuit leading to lethal influenza infection. *Cell* 154:197–212. <https://doi.org/10.1016/j.cell.2013.06.013>.
 39. Petrofsky M, Bermudez LE. 1999. Neutrophils from *Mycobacterium avium*-infected mice produce TNF- α , IL-12, and IL-1 β and have a putative role in early host response. *Clin Immunol* 91:354–358. <https://doi.org/10.1006/clim.1999.4709>.
 40. Fischer MA, Davies ML, Reider IE, Heipertz EL, Epler MR, Sei JJ, Ingersoll MA, Rooijen NV, Randolph GJ, Norbury CC. 2011. CD11b(+), Ly6G(+) cells produce type I interferon and exhibit tissue protective properties following peripheral virus infection. *PLoS Pathog* 7:e1002374. <https://doi.org/10.1371/journal.ppat.1002374>.
 41. Stienstra R, Saudale F, Duval C, Keshtkar S, Groener JE, van Rooijen N, Staels B, Kersten S, Muller M. 2010. Kupffer cells promote hepatic steatosis via interleukin-1 β -dependent suppression of peroxisome proliferator-activated receptor α activity. *Hepatology* 51:511–522. <https://doi.org/10.1002/hep.23337>.
 42. Van Rooijen N, Sanders A. 1996. Kupffer cell depletion by liposome-delivered drugs: comparative activity of intracellular clodronate, propamide, and ethylenediaminetetraacetic acid. *Hepatology* 23: 1239–1243. <https://doi.org/10.1002/hep.510230544>.
 43. Garcia Z, Lemaitre F, van Rooijen N, Albert ML, Levy Y, Schwartz O, Bousso P. 2012. Subcapsular sinus macrophages promote NK cell accumulation and activation in response to lymph-borne viral particles. *Blood* 120:4744–4750. <https://doi.org/10.1182/blood-2012-02-408179>.
 44. Asano K, Nabeyama A, Miyake Y, Qiu CH, Kurita A, Tomura M, Kanagawa O, Fujii S, Tanaka M. 2011. CD169-positive macrophages dominate antitumor immunity by crosspresenting dead cell-associated antigens. *Immunity* 34:85–95. <https://doi.org/10.1016/j.immuni.2010.12.011>.
 45. Probst HC, Tschannen K, Odermatt B, Schwendener R, Zinkernagel RM, Van Den Broek M. 2005. Histological analysis of CD11c-DTR/GFP mice after in vivo depletion of dendritic cells. *Clin Exp Immunol* 141:398–404. <https://doi.org/10.1111/j.1365-2249.2005.02868.x>.
 46. Pearce AF, Lyles DS. 2009. Vesicular stomatitis virus induces apoptosis primarily through Bak rather than Bax by inactivating Mcl-1 and Bcl-XL. *J Virol* 83:9102–9112. <https://doi.org/10.1128/JVI.00436-09>.
 47. Brenner D, Blaser H, Mak TW. 2015. Regulation of tumour necrosis factor signalling: live or let die. *Nat Rev Immunol* 15:362–374. <https://doi.org/10.1038/nri3834>.
 48. Basagoudanavar SH, Thapa RJ, Nogusa S, Wang J, Beg AA, Balachandran S. 2011. Distinct roles for the NF- κ B RelA subunit during antiviral innate immune responses. *J Virol* 85:2599–2610. <https://doi.org/10.1128/JVI.02213-10>.
 49. Marienfeld R, May MJ, Berberich I, Serfling E, Ghosh S, Neumann M. 2003. RelB forms transcriptionally inactive complexes with RelA/p65. *J Biol Chem* 278:19852–19860. <https://doi.org/10.1074/jbc.M301945200>.
 50. Haifinger S, Nogai H, Pelzer C, Jaworski M, Cabalzar K, Charton JE, Guzzardi M, Decaillet C, Grau M, Dorken B, Lenz P, Lenz G, Thome M. 2011. Malt1-dependent RelB cleavage promotes canonical NF- κ B activation in lymphocytes and lymphoma cell lines. *Proc Natl Acad Sci U S A* 108:14596–14601. <https://doi.org/10.1073/pnas.1105020108>.

51. Brustle A, Brenner D, Knobbe CB, Lang PA, Virtanen C, Hershenfield BM, Reardon C, Lacher SM, Ruland J, Ohashi PS, Mak TW. 2012. The NF-kappaB regulator MALT1 determines the encephalitogenic potential of Th17 cells. *J Clin Invest* 122:4698–4709. <https://doi.org/10.1172/JCI63528>.
52. Poeck H, Bscheider M, Gross O, Finger K, Roth S, Rebsamen M, Hanneschlagger N, Schlee M, Rothenfusser S, Barchet W, Kato H, Akira S, Inoue S, Endres S, Peschel C, Hartmann G, Hornung V, Ruland J. 2010. Recognition of RNA virus by RIG-I results in activation of CARD9 and inflammasome signaling for interleukin 1 beta production. *Nat Immunol* 11: 63–69. <https://doi.org/10.1038/ni.1824>.
53. Sghaier I, Zidi S, Mouelhi L, Dabbech R, Ghazouani E, Brochot E, Stayoussef M, Yacoubi-Loueslati B. 2015. The relationship between TNF alpha gene polymorphisms (–238/–308), TNF RII VNTR (p75) and outcomes of hepatitis B virus infection in Tunisian population. *Gene* 568: 140–145. <https://doi.org/10.1016/j.gene.2015.05.029>.
54. Xu J, Zhang S, Zhang Z, Fu L, Zheng Q, Wang J, Lu S, Du J. 2013. TNF-alpha promoter region polymorphisms affect HBV virus clearance in southern Chinese. *Clin Chim Acta* 425:90–92. <https://doi.org/10.1016/j.cca.2013.07.015>.
55. Fletcher NF, Sutaria R, Jo J, Barnes A, Blahova M, Meredith LW, Cosset FL, Curbishley SM, Adams DH, Bertoletti A, McKeating JA. 2014. Activated macrophages promote hepatitis C virus entry in a tumor necrosis factor-dependent manner. *Hepatology* 59:1320–1330. <https://doi.org/10.1002/hep.26911>.
56. Park J, Kang W, Ryu SW, Kim WI, Chang DY, Lee DH, Park DY, Choi YH, Choi K, Shin EC, Choi C. 2012. Hepatitis C virus infection enhances TNFalpha-induced cell death via suppression of NF-kappaB. *Hepatology* 56:831–840. <https://doi.org/10.1002/hep.25726>.
57. Seo SH, Webster RG. 2002. Tumor necrosis factor alpha exerts powerful anti-influenza virus effects in lung epithelial cells. *J Virol* 76:1071–1076. <https://doi.org/10.1128/JVI.76.3.1071-1076.2002>.
58. Ebert G, Preston S, Allison C, Cooney J, Toe JG, Stutz MD, Ojaimi S, Scott HW, Baschuk N, Nachbur U, Torresi J, Chin R, Colledge D, Li X, Warner N, Revill P, Bowden S, Silke J, Begley CG, Pellegrini M. 2015. Cellular inhibitor of apoptosis proteins prevent clearance of hepatitis B virus. *Proc Natl Acad Sci U S A* 112:5797–5802. <https://doi.org/10.1073/pnas.1502390112>.
59. Ebert G, Allison C, Preston S, Cooney J, Toe JG, Stutz MD, Ojaimi S, Baschuk N, Nachbur U, Torresi J, Silke J, Begley CG, Pellegrini M. 2015. Eliminating hepatitis B by antagonizing cellular inhibitors of apoptosis. *Proc Natl Acad Sci U S A* 112:5803–5808. <https://doi.org/10.1073/pnas.1502400112>.
60. Beyer M, Abdullah Z, Chemnitz JM, Maisel D, Sander J, Lehmann C, Thabet Y, Shinde PV, Schmidleithner L, Kohne M, Trebicka J, Schierwagen R, Hofmann A, Popov A, Lang KS, Oxenius A, Buch T, Kurts C, Heikenwalder M, Fatkenheuer G, Lang PA, Hartmann P, Knolle PA, Schultze JL. 2016. Tumor-necrosis factor impairs CD4(+) T cell-mediated immunological control in chronic viral infection. *Nat Immunol* 17: 593–603. <https://doi.org/10.1038/ni.3399>.
61. Faber M, Bette M, Preuss MA, Pulmanusahakul R, Rehne J, Schnell MJ, Dietzschold B, Weihe E. 2005. Overexpression of tumor necrosis factor alpha by a recombinant rabies virus attenuates replication in neurons and prevents lethal infection in mice. *J Virol* 79:15405–15416. <https://doi.org/10.1128/JVI.79.24.15405-15416.2005>.
62. Junt T, Scandella E, Ludewig B. 2008. Form follows function: lymphoid tissue microarchitecture in antimicrobial immune defence. *Nat Rev Immunol* 8:764–775. <https://doi.org/10.1038/nri2414>.
63. Bernhard CA, Ried C, Kochanek S, Brocker T. 2015. CD169+ macrophages are sufficient for priming of CTLs with specificities left out by cross-priming dendritic cells. *Proc Natl Acad Sci U S A* 112:5461–5466. <https://doi.org/10.1073/pnas.1423356112>.
64. Moseman EA, Iannaccone M, Bosurgi L, Tonti E, Chevrier N, Tumanov A, Fu YX, Hacohen N, von Andrian UH. 2012. B cell maintenance of subcapsular sinus macrophages protects against a fatal viral infection independent of adaptive immunity. *Immunity* 36:415–426. <https://doi.org/10.1016/j.immuni.2012.01.013>.
65. Lenardo MJ, Fan CM, Maniatis T, Baltimore D. 1989. The involvement of NF-kappa B in beta-interferon gene regulation reveals its role as widely inducible mediator of signal transduction. *Cell* 57:287–294. [https://doi.org/10.1016/0092-8674\(89\)90966-5](https://doi.org/10.1016/0092-8674(89)90966-5).
66. Hiscott J, Alper D, Cohen L, Leblanc JF, Sportza L, Wong A, Xanthoudakis S. 1989. Induction of human interferon gene expression is associated with a nuclear factor that interacts with the NF-kappa B site of the human immunodeficiency virus enhancer. *J Virol* 63:2557–2566.
67. Wang X, Hussain S, Wang EJ, Li MO, Garcia-Sastre A, Beg AA. 2007. Lack of essential role of NF-kappa B p50, RelA, and cRel subunits in virus-induced type 1 IFN expression. *J Immunol* 178:6770–6776. <https://doi.org/10.4049/jimmunol.178.11.6770>.
68. Wang J, Basagoudanavar SH, Wang X, Hopewell E, Albrecht R, Garcia-Sastre A, Balachandran S, Beg AA. 2010. NF-kappa B RelA subunit is crucial for early IFN-beta expression and resistance to RNA virus replication. *J Immunol* 185:1720–1729. <https://doi.org/10.4049/jimmunol.1000114>.
69. Wang X, Wang J, Zheng H, Xie M, Hopewell EL, Albrecht RA, Nogusa S, Garcia-Sastre A, Balachandran S, Beg AA. 2014. Differential requirement for the IKKbeta/NF-kappaB signaling module in regulating TLR- versus RLR-induced type 1 IFN expression in dendritic cells. *J Immunol* 193: 2538–2545. <https://doi.org/10.4049/jimmunol.1400675>.
70. Jin J, Hu H, Li HS, Yu J, Xiao Y, Brittain GC, Zou Q, Cheng X, Mallette FA, Watowich SS, Sun SC. 2014. Noncanonical NF-kappaB pathway controls the production of type I interferons in antiviral innate immunity. *Immunity* 40:342–354. <https://doi.org/10.1016/j.immuni.2014.02.006>.
71. Ruland J, Duncan GS, Wakeham A, Mak TW. 2003. Differential requirement for Malt1 in T and B cell antigen receptor signaling. *Immunity* 19:749–758. [https://doi.org/10.1016/S1074-7613\(03\)00293-0](https://doi.org/10.1016/S1074-7613(03)00293-0).
72. Oetke C, Vinson MC, Jones C, Crocker PR. 2006. Sialoadhesin-deficient mice exhibit subtle changes in B- and T-cell populations and reduced immunoglobulin M levels. *Mol Cell Biol* 26:1549–1557. <https://doi.org/10.1128/MCB.26.4.1549-1557.2006>.
73. Jung S, Unutmaz D, Wong P, Sano G, De los Santos K, Sparwasser T, Wu S, Vuthoori S, Ko K, Zavala F, Pamer EG, Littman DR, Lang RA. 2002. In vivo depletion of CD11c+ dendritic cells abrogates priming of CD8+ T cells by exogenous cell-associated antigens. *Immunity* 17:211–220. [https://doi.org/10.1016/S1074-7613\(02\)00365-5](https://doi.org/10.1016/S1074-7613(02)00365-5).
74. Miyake Y, Asano K, Kaise H, Uemura M, Nakayama M, Tanaka M. 2007. Critical role of macrophages in the marginal zone in the suppression of immune responses to apoptotic cell-associated antigens. *J Clin Invest* 117:2268–2278. <https://doi.org/10.1172/JCI31990>.
75. Iwata A, Nishio K, Winn RK, Chi EY, Henderson WR, Jr, Harlan JM. 2003. A broad-spectrum caspase inhibitor attenuates allergic airway inflammation in murine asthma model. *J Immunol* 170:3386–3391. <https://doi.org/10.4049/jimmunol.170.6.3386>.
76. Hotchkiss RS, Chang KC, Swanson PE, Tinsley KW, Hui JJ, Klender P, Xanthoudakis S, Roy S, Black C, Grimm E, Aspiotis R, Han Y, Nicholson DW, Karl IE. 2000. Caspase inhibitors improve survival in sepsis: a critical role of the lymphocyte. *Nat Immunol* 1:496–501. <https://doi.org/10.1038/82741>.